THE EUROPEAN

Martian CLIMATE DATABASE

for mission planning & for scientific studies

F. Forget, R. Fournier, C. Hourdin, F. Hourdin and O. Talagrand
(Laboratoire de Météorologie Dynamique, CNRS-UPCM, Paris, France)

M. Collins, S.R. Lewis and P.L. Read
(Atmospheric, Oceanic and Planetary Physics, Clarendon Laboratory, Oxford, UK)

J.-P. Huot
(Analyse de l'environnement des systemes spatiaux, ESTEC, Noordwijk, Netherlands)

Contents

1 Introduction

A database of statistics on the climate and environment of the Martian atmosphere has been constructed jointly by two european teams from LMD (Paris) and AOPP (Oxford), with the support of the European Space Agency (ESTEC TRP contract 11369/95/NL/JG). This database was primarily designed to provide information about the planetary environment to the engineers preparing spacecraft missions operating in this environment.

Previous so-called "engineering models" (e.g. "MarsGRAM") used for that purpose were based on compilations of observational statistics with simple interpolation schemes to provide estimates of climate variables at any time and any geographical location. Unfortunately, the available observational data on Mars are very sparse and incomplete in both space and time, leading to great uncertainties for locations, times and seasons for which no data is available.

A different approach has been used here. The database has been produced from a set of carefully validated simulation of Mars's climate and atmospheric circulation conducted with a General Circulation Model (GCM). GCMs are widely used for weather forecasting and climate studies for the Earth. In particular, the GCM "analysis" which are produced by the meteorological centers from a combination of model calculations and observations are more and more used as a reference climatology. Several GCMs have been succesfully adapted to to the Martian conditions. The GCM which have been used here is based on the suites of models adapted to Mars a few years ago at LMD and AOPP. In preparation for producing the database, a number of enhancement have been made to these earlier models. The resulting GCM, and the database compiled with it are now believed to be state-of-the art tools to describe and study the Martian environment.

2 Martian General Circulation Model

2.1 General features

General Circulation Models can be schematically divided into two parts.

- The first part is an **hydrodynamical code** dedicated to the time and spatial integration of the equations of hydrodynamics. This part, based on a rather general formulation of the equations of fluid mechanics (primitive equations in meteorological dialect) can be used without any change for the other terrestrial planets. Two different kind of hydrodynamical code have been developed so far: 1. finite-differences or grid-points models (on use at LMD) and 2. spectral solver based on a decomposition of the horizontal fields on spherical harmonics (on use at AOPP).

- The second part of the code consists of a set of **physical parametrizations**, among which **radiative transfer**, which is the source of atmospheric motions (principally the latitudinal variations of the absorption of solar energy), plays a central role. Since radiative transfer must be computed several times a day (when one wants to explicitly represent the diurnal cycle) on an horizontal grid made of thousands of points and typically a few tens of meshes on the vertical, the numerical code must be very efficient. A number of approximations must be introduced depending on the specific planetary conditions. Adaptation of a radiative transfer code is thus usually the main step in the development of an atmospheric GCM for other planetary atmospheres.

The physical parametrizations must also include representation of small scale motions not explicitly represented by the hydrodynamical code. Among those small scale processes, the most important is the representation of vertical exchange of momentum and energy between the surface and the atmosphere in the so-called **Planetary Boundary Layer**.

Finally, a number of planet-specific parametrizations must be included such as the various components of the hydrological cycle on Earth (vegetation, clouds and precipitation). On Mars, as will be explained below, representation of condensation and sublimation of atmospheric CO_2 is essential for a realistic representation of the pressure cycle.

2.2 Martian atmospheric GCM's through time

As early as in the late sixties, the then recently developed Terrestrial GCM of UCLA was successfully adapted to Martian conditions by Leovy and Mintz (1969). The model predicted atmospheric condensation of CO_2 and the presence of transient baroclinic waves in the winter mid -latitudes, facts which have since been confirmed by spacecraft exploration. The same model was developed further by the NASA/Ames group and has provided a number of keys for our understanding of the Martian climate (see e.g., Pollack et al., 1982, Haberle et al., 1993).

In 1989, the LMD GCM was adapted to Mars by developing a new radiative transfer code (Hourdin, 1992) and a self-consistent parametrization for the condensation and sublimation of CO_2. This model was the first one to simulate one ever to simulate a full Martian year without any other forcing than insolation (Hourdin et al., 1993, 1995). It was able to reproduce in a very satisfactory way the seasonal pressure variations observed by the Viking landers.

More recently, a similar effort was developed jointly at Reading University and Oxford. A spectral solver was used in conjunction with a simplified version of the physical parametrizations. Original results were obtained on the dynamical regime of baroclinic waves (Collins and James, 1995) and on the boundary-current nature of the low cross-equatorial branch of the Hadley circulation (Joshi et al., 1994).

At about the same time, a new grid point model was developed at the Geophysical Fluid Dynamic Laboratory (GFDL, USA) with inclusion of a sophisticated physical package. It has been used for the study of thermal tides (Wilson and Hamilton, 1996).

Within that context, and with the support of the European Space Agency, the LMD and Oxford groups have joined their efforts in order to develop a new generation Martian GCM.

2.3 A European Martian GCM

The GCM which has been used for the construction of the climate database includes the two hydrodynamical codes of LMD and Oxford and a very sophisticated set of physical parametrizations built on that originally developed for the LMD GCM (Hourdin et al. 1993), and largely enhanced in preparation for the producing the database.

The **radiative transfer code** in the infrared includes The absorption and emission by carbon dioxide, computed using the scheme developed by Hourdin (1992). It also accounts for scattering by the dust in addition to absorption and emission. The treatment of the dust is based on the algorithm developed by Toon et al. (1989). At solar wavelengths, besides dust absorption and scattering, a simple parametrization for the computation of the near infrared heating by CO_2 gas, which is negligible below 30km but becomes considerable above 50km, has been included. The **dust optical properties** are derived from Ockert-Bell et al. (1997) in the solar wavelengths, and from an improved version of the Toon et al. (1977) model in the infrared. Following Martin (1986) and Clancy et al. (1995), the visible (0.67 μm) to infrared (9 μm) dust optical depth ratio has been set to 2.

The formulation of the **vertical turbulent mixing** (mainly of importance in the **planetary boundary layer**) has been improved based on a second-order closure scheme of Mellor and Yamada (1974) type. Such a sophisticated scheme improves the representation of the mean near surface wind, and allows to predict temperature and wind standard deviations, which are of primary importance for analysis of the low atmosphere conditions.

In addition to this parametrization, a **convective adjustment scheme** is used to prevent subadiabatic vertical temperatures gradients.

The temperature of the surface is computed from the radiative, sensible and latent heat fluxes at the surface using an 11-level model of **thermal diffusion in the soil**. Surface properties, i.e. **albedo** and thermal inertia, are based on the Viking observations analyzed by Pleskot and Miner (1982) and Palluconi and Kieffer (1981), completed in the polar regions by the recent results from Paige et al. (1994) and Paige and Keegan (1994). We have used the **USGS Digital Elevation Map** (often called DTM) for the topography.

In fact, the orography used in GCM's is smoothed to the horizontal resolution of the model. Variations of orography below the grid scale are ignored. These sub-grid scale variations can, however, have a significant impact on the circulation of the atmosphere : The sub-grid scale mountains can influence the model scale flow by (a) producing a form drag on the flow at low levels, and by (b) exciting internal gravity waves which can propagate in the vertical, break, and decelerate the flow far away from the mountains themselves. These two effects have been parametrised using, for (a), the **low level drag scheme** of Lott and Miller (1996) and for (b) the **gravity wave drag scheme** of Miller et al. (1989) and Baines and Palmer (1990).

Last but not least, a specific parametrization has been developed for Mars to account for the **condensation of the CO_2 atmosphere** in the polar region during the polar night seasons. CO_2 can condense directly on the surface or up in the atmosphere. In that last case, the CO_2 ice particles formed in the atmosphere are thought to affect the radiative balance of the polar regions and thus the total amount of CO_2 which condenses in the polar caps (Forget and

Pollack, 1995). This effect has been included in the model by predicting a decrease of the surface emission to space depending on the quantity of CO_2 condensed in the atmosphere.

In oder to produce the database, the spatial resolution has been increased. The horizontal resolution adopted for the database is smaller than 220 km everywhere, with a vertical discretisation of 25 layers extending from the surface up to about 90 km.

3 Comparison with observations

The key features of the Martian environment observed by the spacecraft missions of the 1970's, Mariner 9 and Viking, can be quantitavely compared with results from the General Circulation Models and in particular with the data contained in the Martian Climate Database described in the present document.

- **Surface pressure.** Figure 1 shows the Viking 1 and 2 daily averaged surface pressure observations taken from the first year of the mission and the corresponding curves simulated by the GCM, as represented in the database (details below). The large seasonal cycle is due to mainly to the condensation and sublimation of CO_2 while the high frequency oscillations are due to weather systems passing over the landers.

- **Temperature.** There is scanty data on atmospheric temperature. The only *in situ* observations were obtained during the entry of the Viking Landers in 1976. Figure2 shows temperature measurements taken during the entry phase of the Viking lander 2, compared with the temperature profile simulated by the GCM at the same date and location.

  In fact, the majority of temperature observations of the Martian atmosphere come from remote sensing of the atmosphere by instruments aboard orbiting spacecraft. Figure 3 shows a comparison of the temperatures field derived by Leovy (1982) from the Mariner 9 IRIS instrument measurements during northern spring with GCM simulations performed for a relatively clear and dusty (for the season) atmosphere (see details on the dust scenario below). The atmospheric temperatures are indeed primarily controlled by the amount of airborne dust, which is highly variable spatially, seasonally and from year to year.

- **Wind.** Direct observations of winds on Mars are extremely rare (Zurek *et al.*, 1992). However, winds have been inferred from a variety of secondary effects, such as streak features on the Martian surface (Magalhaes, 1987). These observations suffer from the problems of incomplete global coverage and uncertainties in the understanding of exactly how and when the features were formed. Figure 4 shows a comparison between some wind directions inferred from wind streak data with low level winds from the GCM. Although there exist some uncertainties in the appropriate dust loading, range of times to average over and heights to sample the winds at, some similarities does appear. In particular, both zonally-averaged diagrams show evidence of predominant westerlies at high northern latitudes, a region of north-easterlies north of the equator with rotation back to westerlies in the southern midlatitudes. There are also similarities

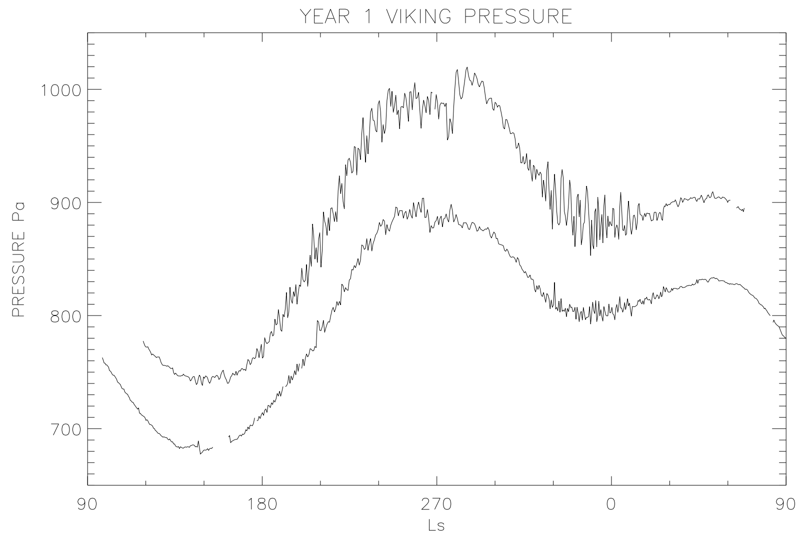

(a) **Viking Observations**

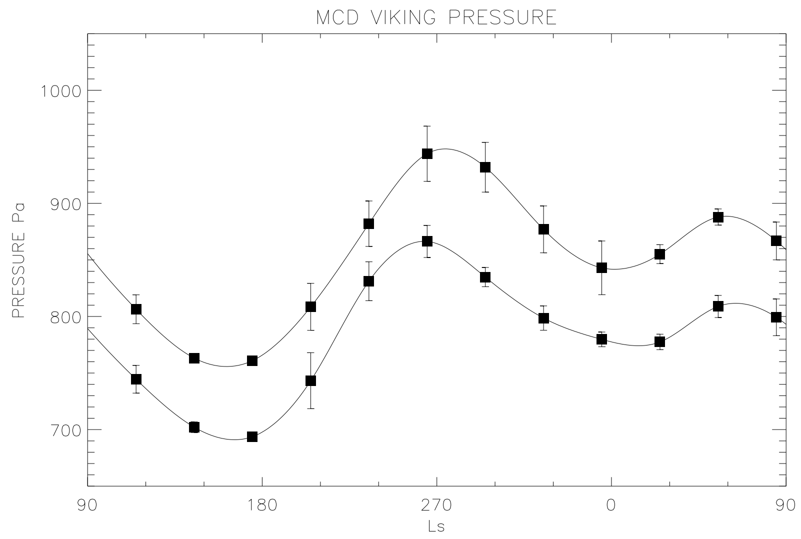

(b) **Database (GCM simulation)**

Figure 1: *Observed and simulated pressures at the Viking Lander sites during the first year of the mission (Viking 1: lower curve, Viking 2: upper curve). The black squares show the database diurnally averaged seasonal values and intervals of* $30° L_s$ *and the smooth curve is a cubic spline fit to these values. In the observations, the high frequency oscillations are due to weather systems passing over the landers. They are well simulated by GCMs (Hourdin et al., 1995, Collins et al., 1996). They are represented here by the error bars which indicate twice the standard deviation of pressure.*

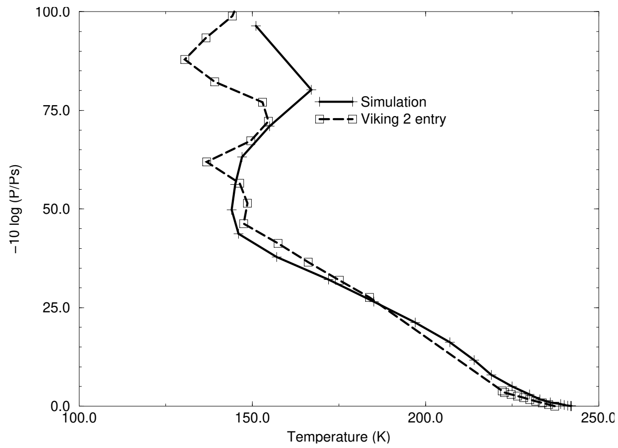

Figure 2: *Viking Lander 2 entry temperature profile compared with the simulation (for the simulation, the points correspond to the model discretisation)*

in the wind and streak directions in the longitude–latitude maps in several regions where there are observations. The difficulties in interpretation of the streak data make a strict comparison impossible, but the GCM results winds seem at least plausible.

- **Polar Caps** Figure 5 shows the time-mean equivalent latitudes for the edges of the polar caps of carbon dioxide ice for the the four scenarios from the Martian Climate Database (see below). The equivalent latitude is that which would be reached by a perfectly symmetrical cap occupying the same area as the total area of ice coverage in that hemisphere. Also shown are actual observations of the edges of the Martian ice caps only available during the spring. The agreement appears reasonable.

4 Database structure and use

4.1 Contents and grid structure

The database contains the following variables :

Variable	symbol	units	2-D or 3-D
CO_2 ice cover	co2ice	$kg\, m^{-2}$	2-D
Surface emissivity	emis	none	2-D
Surface temperature	tsurf	K	2-D
Surface pressure	ps	Pa	2-D
Atmospheric temperature	t	K	3-D
Zonal (east-west) wind	u	$m\, s^{-2}$	3-D
Meridional (north-south) wind	v	$m\, s^{-2}$	3-D
Atmospheric density	rho	$kg\, m^{-3}$	3-D
Boundary layer eddy kinetic energy	q2	$m^2\, s^{-2}$	3-D

These variables are written on an equally spaced horizontal grid of 96 east longitude points numbered from 0° to 356.25° in steps of 3.75° and 48 latitude points numbered from −88.125°

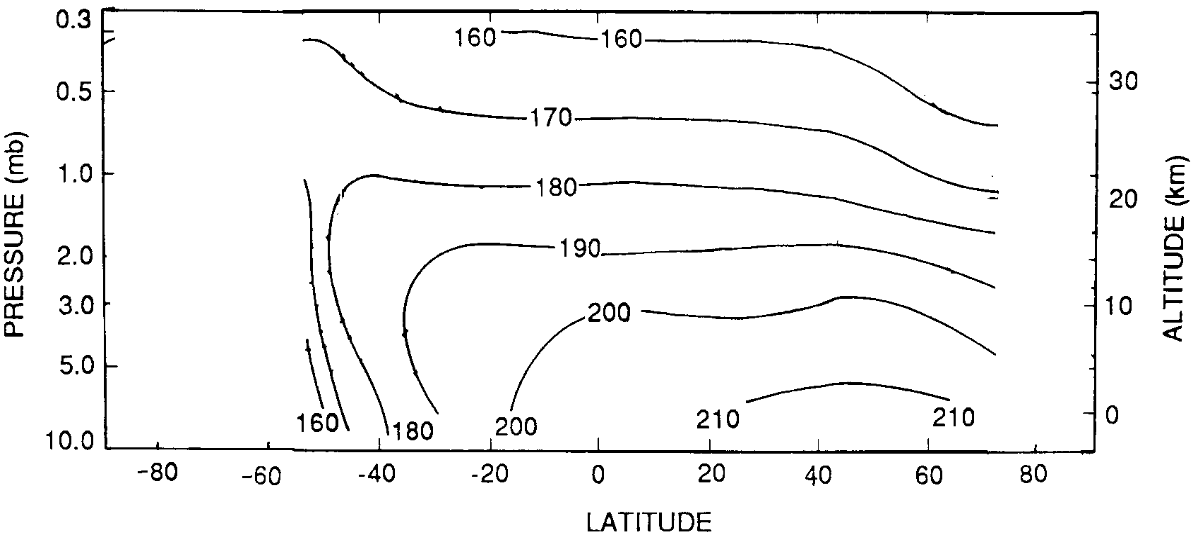

(a) Temperature (K) observed by Mariner 9 IRIS ($L_s = 43^o - 54^o$)

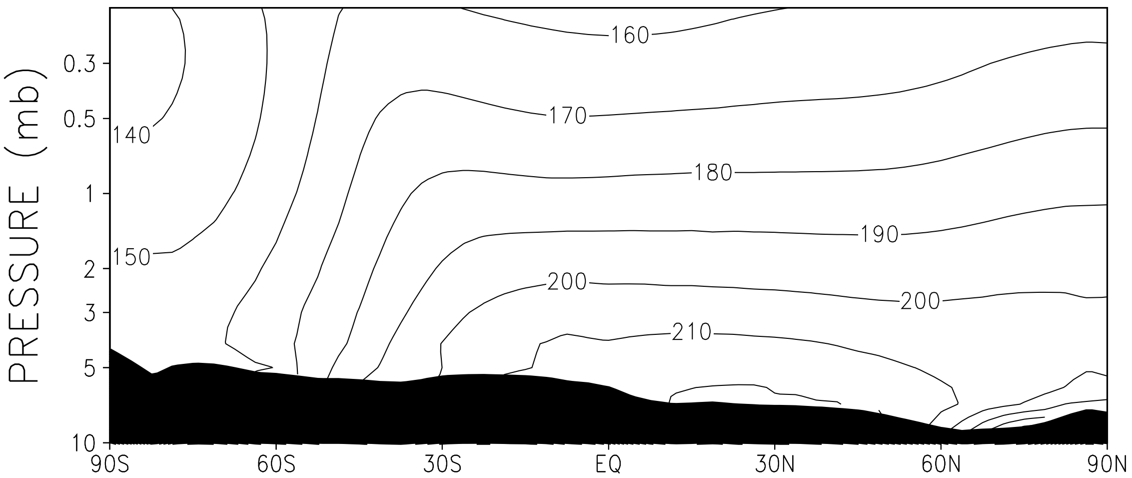

(b) T (K) simulated by the GCM : clear year scenario

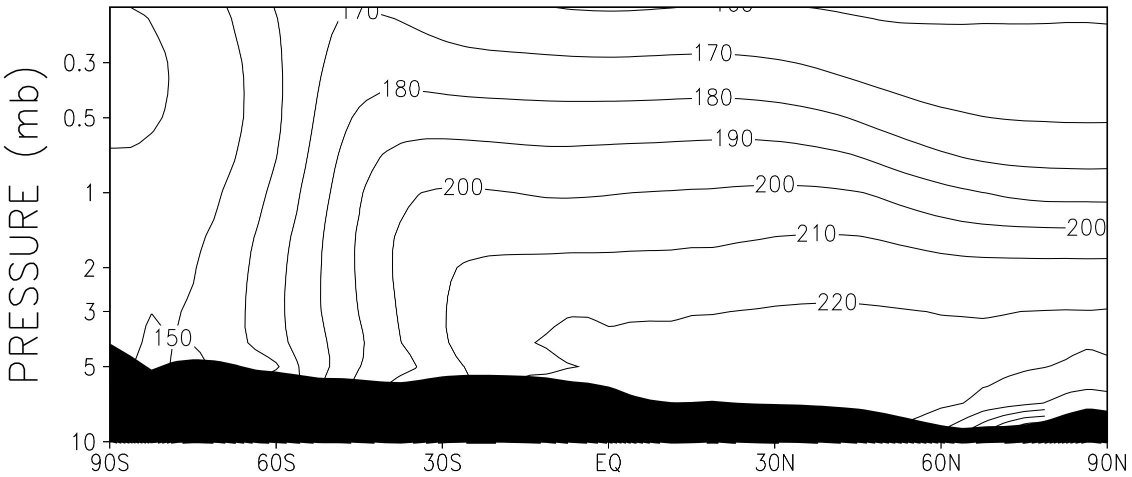

(c) T (K) simulated by the GCM : Viking year scenario ("dusty year")

Figure 3: *The thermal structure observed by Mariner 9 IRIS in 1972 (from Leovy, 1982) during northern spring ($L_s = 43^o - 54^o$), compared to the zonal averaged temperatures simulated by the GCM for the same period. The spring observed by Mariner 9 is known to have been clearer (and colder) than the spring observed by Viking (Clancy et al., 1996). This is reflected here.*

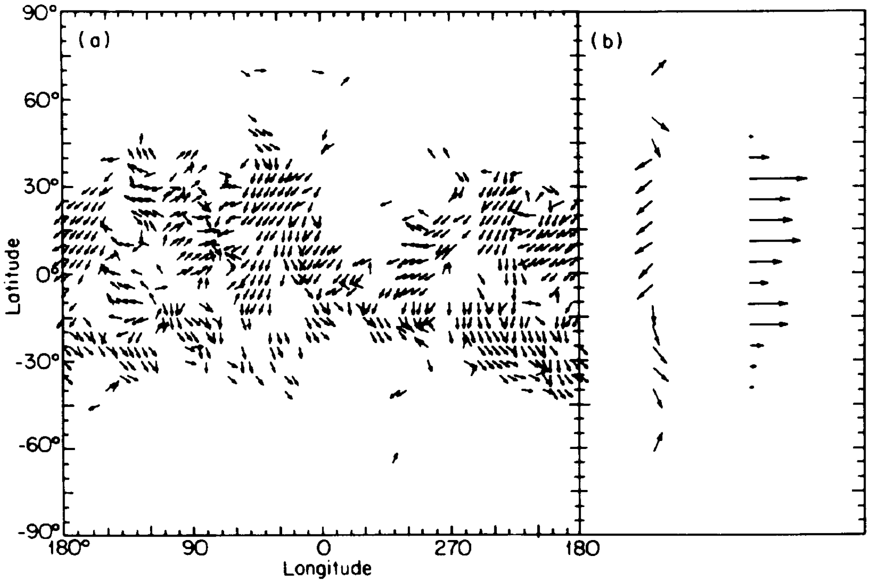

(a) **Wind surface streaks observations**

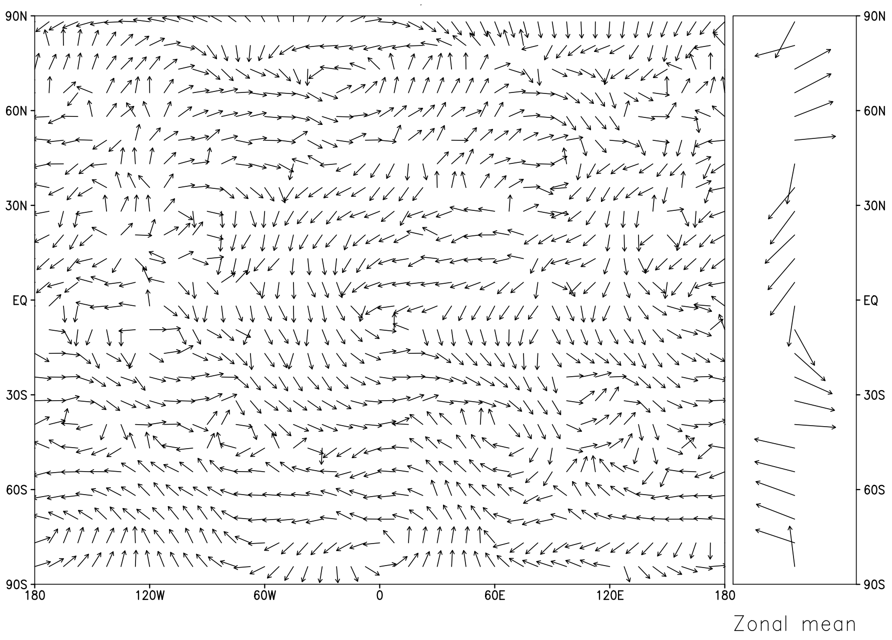

(b) **GCM database lower level winds directions**

Figure 4: ***Above:*** *Distribution of "Type I(b)" surface streak orientations derived from Viking Orbiter mosaics (from Magalhaes, 1987): (a) average azimuths for 5°×5° bins; (b) zonally averaged azimuths in 2° bins (every fourth bin shown), with horizontal arrows representing the relative number of streaks in each bin, the longest of which represents 700 streaks. The "Type I(b)" streaks are thought to indicate the directions of near-surface winds during the decay of the global dust storms in 1977. They can be compared to the mean winds directions simulated in the lowest level of the GCM (**Below**) over the corresponding season L_s = 270°– 300°, for dust storm conditions (dust opacity $\tau = 2$). Only every second point in each direction is shown for clarity.*

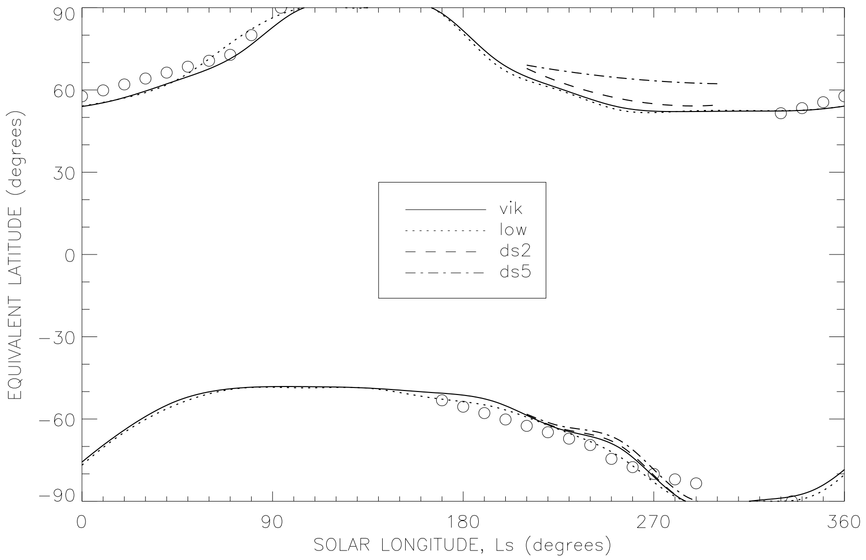

Figure 5: *Mean equivalent latitudes for the edges of the polar caps of carbon dioxide ice for the four scenarios from the Martian Climate Database, labelled according to the usual convention. The circles indicate actual observations of the edges of the Martian caps, kindly provided by J.B. Pollack (priv. com.).*

to 88.125° in steps of 3.75°. The vertical coordinate for the 3D variables is defined as

$$\sigma = \frac{p}{p_*} \tag{1}$$

where p is the atmospheric pressure and p_* is the surface pressure. Thus σ is 1 at the surface and 0 at infinity and the σ levels follow the model orography. There are 25 sigma levels, with the first three level are at about 5, 19 and 44 m whereas the upper level is around 95 km.

Fields are averaged and stored 12 times a day, for 12 Martian "seasons" to give a **comprehensive representation of the annual and diurnal cycles**. Each season covers 30^o in solar longitude (L_s), and are typically 50-70 days long.

4.2 Dust distribution scenarios in the Martian climate database

The overall intention of the Database is to provide guidance on the typical state of the Martian climate system and its associated variability, in a way which represents knowledge not only from direct observations, but also from *a priori* knowledge of the dynamic and physics of the Martian atmosphere and surface. Despite the sparseness of observations, it is already clear that the Martian climate system at present exhibits a range of quite different states from year to year, ranging from the very clear and cold conditions encountered for instance during the recent Phobos mission to the very dusty conditions observed by Viking (see Clancy et al., 1996). In order to represent these long-term variations, the database includes results from several different "dust distribution scenarios".

- A seasonally-varying dust (atmospheric optical depth $\tau = 0.7 + 0.3\cos(L_s + 80^o)$) as observed during the dusty Viking Lander years (Colburn et al., 1989), but with the large dust storms removed. The dust distribution in the vertical varies as a function of both time and latitude, as observed by the Viking cameras (Jaquin et al., 1986).

- A low, uniform dust ($\tau = 0.1$), appropriate to more recent observations of a clearer, colder Mars.

- In addition, scenarios were conducted for several seasons with much higher dust loadings ($\tau = 2$ and $\tau = 5$), appropriate to dust storm conditions.

4.3 Representing the variability

Mean fields are stored in the database once a season. Although the main variability, which is due to the diurnal cycle, is captured by storing the fields 12 times a day, there may still be significant variation about the mean due to, for example, motions of baroclinic weather systems.

- **Large scale variability** in the database is represented using a novel approach based on a technique that is widely used in meteorological data analysis as well as in other subject areas, using Empirical Orthogonal Functions (EOFs). Let $D(z)$ be the database mean vertical profile of a meteorological variable. We add a series of functions to the mean vertical profile,

$$D(z) = \overline{D}(z) + \sum_{n=1}^{N} p_i e_i(z) \qquad (2)$$

  where the functions e_i are eigenvectors of the covariance matrix of the modelled profiles (the EOFs) and p_i are the amplitudes of the functions (the Principal Components). The e_i form an optimal linear basis such that the variance captured is high even when the truncation limit is low. In order to retain cross-correlations in altitude between different variables we combine all the variables together and form a set of multivariate functions. In practice the series (2) is truncated to 6 EOFs which, on average, capture around 80-90% of the variance.

- A **small scale variability model**, simulating perturbations of density, temperature and wind due to the upward propagation of small scale gravity waves have been included in the database system. The model is based on the parametrization scheme used the numerical models that simulated the data in the database.

4.4 Accessing data

In practice, there are three main ways of accessing data from the MCD which have currently been implemented.

- Firstly, a complete interface, MCDGM, is supplied with the Mars Climate Database. The MCDGM interface performs in a very similar way to MarsGRAM version 3.5. It is

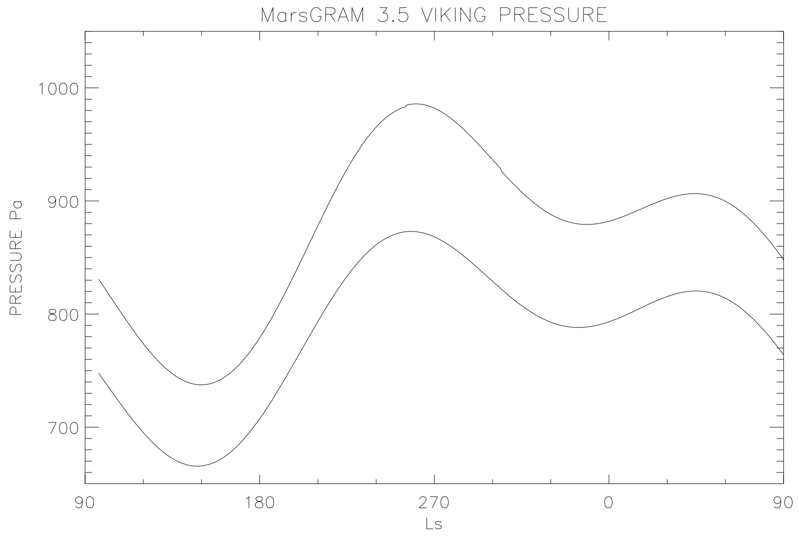

Figure 6: *MarsGRAM Viking 1 (lower curve) and 2 (upper curve) surface pressure for one Martian year.*

intended to make the database as easy to use as possible for those with prior experience of MarsGRAM as well as providing straightforward access for all users to the complete database, including the variability model and orographic wave model. It can be run in interactive or batch mode.

- Secondly, it is possible to access the database directly from within any program, written in FORTRAN or C, by using the Data Retrieval and Storage (DRS) library. Indeed, The data in the database is written using the Data DRS library developed for the Program for (Terrestrial) Climate Model Diagnosis and Intercomparison (PCMDI) easily available. This gives the most flexibility for particular applications, although it does demand a greater understanding of how the database and variability models, if they are required, should be used.
- Thirdly, control files, instructions and example scripts are provided for accessing the database using GrADS. GrADS is a freely available package for access, manipulation and display of earth science data which runs on many computing platforms. This provides a very easy method of examining and plotting mean and standard deviation data from the MCD in a variety of formats.

A full documentation including a complete *User Manual* is available. A **World Wide Web** site is beeing developed at LMD (http://www.lmd.jussieu.fr/mars.html). In adition to a complete documention, the site will offer an alternative way to access the data.

5 Comparison with MarsGRAM v3.5

Mars-GRAM being based on a compilation of the available observations, the comparison of its results with these observations is obviously satisfactory. However, the extrapolation to

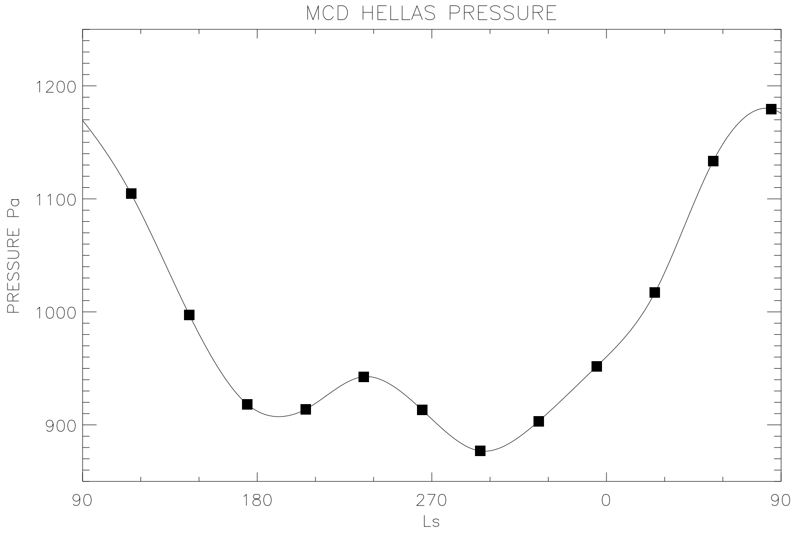

(a) **GCM Martian Database)**

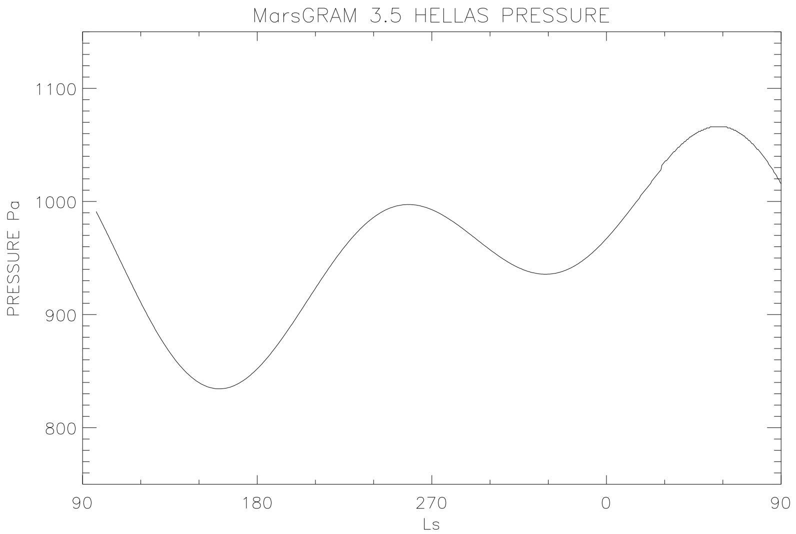

(b) **MarsGRAM)**

Figure 7: *Surface pressure given by the Martian GCM database and by MarsGRAM for one Martian year at longitude* 300° *west, latitude* 40° *south, i.e. the Hellas basin. The black squares show the MCD diurnally averaged seasonal values and intervals of* $30° L_s$ *and the smooth curve is a cubic spline fit to these values.*

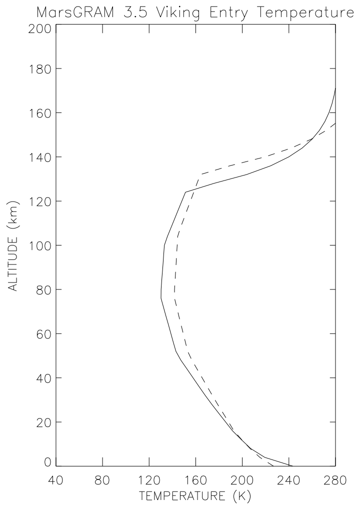

Figure 8: MarsGRAM Viking 1 (solid) and Viking 2 (dashed) entry temperature profiles.

other seasons, dust conditions or locations is based on some a priori functions which are not constraint by observations.

At the opposite, the extrapollation done by the GCM is based on physical processes fully accounted for in the model. Therefore the comparison between Mars-GRAM, the GCM climate database and the observations can be summarized as follows: when observations are available, the GCMMCD gives almost as good results as Mars-GRAM does. For other locations, Mars-GRAM and the GCMMCD gives significantly different results but, in that case, the GCMMCD results are likely to be more reliable.

This is illustrated in some examples bellow.

- **Surface Pressure.**

  Figure 6 shows the MarsGRAM v3.5 surface pressure from the Viking lander locations for one year. The agreement with the observed pressure (fig. 1) is very good as Mars-GRAM fits a functional form to the observed seasonal pressure. However MarsGRAM provides no information on the synoptic variability whereas the MCD does. Also it must be noted that not all the seasonal cycle in pressure is due to the condensation-sublimation cycle. Under certain circumstances there can be a significant component due to density gradients within the atmosphere (the dynamical component). This phenomenon shows up when looking at seasonal pressure curves from other points on the planet. Figure 7 shows the daily averaged pressure taken from the Hellas basin (longitude 300° west, latitude 40° south) from the MCD and from MarsGRAM. There is a marked difference in the seasonal pressure cycle compared to the pressure cycles at the Viking sites due to the dynamical component. This is one of the key advantages of using the MCD rather than just fitting seasonal pressure curves from the observed Viking data.

(a) Temperature (K) observed by Mariner 9 IRIS (L_s = 43°– 54°)

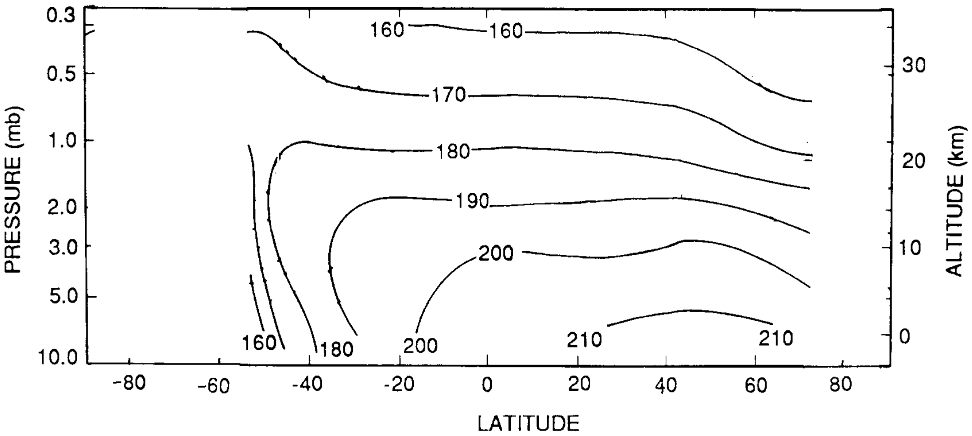

(b) Temperature (K) from MarsGRAM

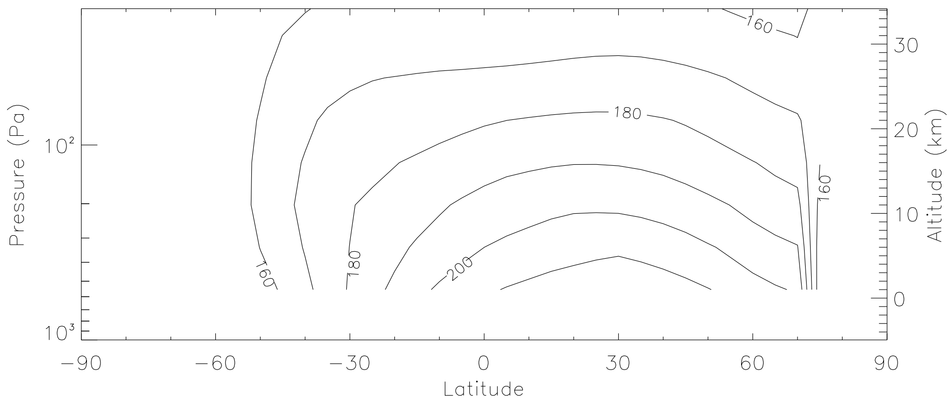

Figure 9: The thermal structure observed by the IRIS instrument on board Mariner 9 in 1972 (from Leovy, 1982) during northern spring (L_s = 43°– 54°), compared to the zonally averaged temperatures from MarsGRAM.

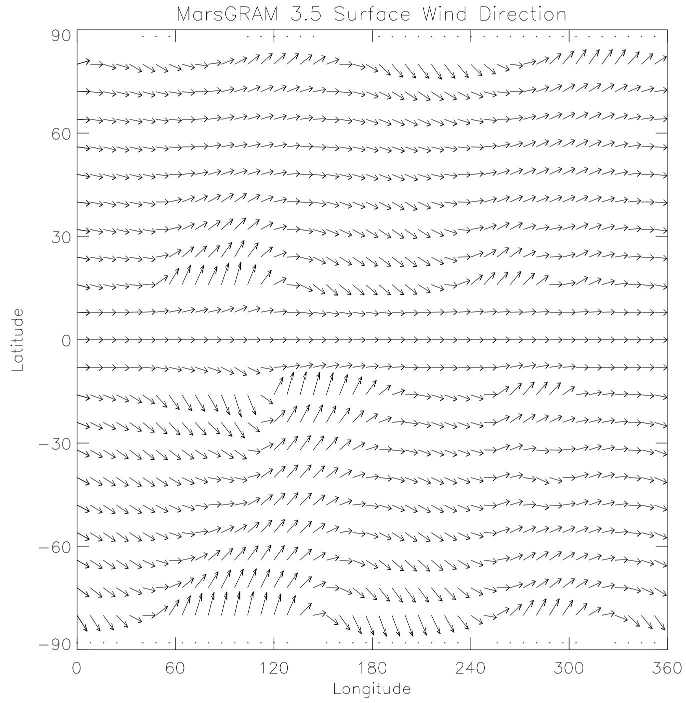

Figure 10: *Winter near-surface wind direction from MarsGRAM, to be compared with Fig. 4.*

- **Temperature.** Figure 8 shows the MarsGRAM v3.5 simulated Viking entry temperature profiles to be compared with the observations and the MCD profiles shown in figure 2. Again, MarsGRAM has a good agreement with the mean profile but has no representation of variability. One of the key advantages of MarsGRAM in this case is that it extents upwards of 90km where the MCD has no information, however the agreement with observations is not particularly good in these regions.

  The comparison of MarsGRAM v3.5 and the Mariner 9 IRIS temperatures from Leovy (1982) is shown in figure 9. The comparison is very good, especially at upper levels where MarsGRAM captures the cold temperatures at this less dusty season. The agreement is less good towards the north polar regions where MarsGRAM predicts a strong horizontal gradient in temperature. However, this good agreement is probably due to the fact that in MarsGRAM temperatures a derived using a fit to these observations. The MCD has not been optimised in such a way (the dust distributions, which to a large extent fixes the vertical temperature gradient, have been chosen to represent a wide range of possible conditions on Mars, not the specific observational conditions) so the fit could only be good to a first approximation.

- **Winds.**

  In the absence of direct information on the martian winds, the winds provided by MarsGRAM (e.g. Fig. 10) are very different from the ones simulated by the GCM (see Fig. 4), and probably not reliable.

6 Conclusion

A new Mars Climate Database (MCD) has been developped with the support of the European agency. The Database is broadly consistent with all the available observational data. Compared with the most commonly used engineering model of Mars - MarsGRAM -, the strength of the MCD is that it provides a physically consistent view of the environmental conditions on Mars for the seasons and dust loadings that are not covered by the observations. Hence the MCD may be thought of as the best current estimate of the environmental conditions on Mars.

Nevertheless, the general circulation model and the database system itself should improve in the future. Large uncertainties in our current understanding and representation of the Martian environment remains, due to the fact that the Martian topography has not yet been accurately measured or that the dust distribution in the atmosphere is poorly known. These particular points, and many others, should be improved in the near future thanks to the observations from Mars Global Surveyor in 1998. Also, to improve our knowledge of the dust cycle and better simulate the related environmental changes, it is planned to incorporate the lifting and transport of the dust in the GCM. It is also planned to extend the altitude of the model up to at least 120 km, to remove potential contamination by boundary conditions in the upper levels of the model. Besides, in the light of feedback from users of the first version of the Martian Database, improvements will be made where desirable.

References

[Baines and Palmer, 1990] Baines, P. G. and Palmer, T. N. (1990). Rationale for a new physically-based parametrisation of sub-grid scale orographic effects. Technical Report 169, ECMWF.

[Clancy et al., 1996] Clancy, R., Grossman, A. W., Wolff, M. J., James, P. B., Rudy, D. J., Billawala, Y. N., Sandor, B. J., Lee, S. W., and Muhleman, D. O. (1996). Water vapor saturation at low altitudes around Mars aphelion: a key to Mars climate. *Icarus*, 122:36–62.

[Clancy et al., 1995] Clancy, R. T., Lee, S. W., Gladstone, G. R., McMillan, W. W., and Rousch, T. (1995). A new model for Mars atmospheric dust based upon analysis of ultraviolet through infrared observations from Mariner 9, Viking, and Phobos. *J. Geophys. Res.*, 100:5251–5263.

[Colburn et al., 1989] Colburn, D. S., Pollack, J. B., and Haberle, R. M. (1989). Diurnal variations in optical depth at Mars. *Icarus*, 79:159–189.

[Collins and James, 1995] Collins, M. and James, I. N. (1995). Regular and irregular baroclinic waves in a simplified global circulation model of the martian atmosphere. *J. Geophys. Res.*, 100(E7):14421–14432.

[Collins et al., 1996] Collins, M., Lewis, S. R., Read, P. L., and Hourdin, F. (1996). Baroclinic wave transitions in the martian atmosphere. *Icarus*, 120:344–357.

[Forget et al., 1995] Forget, F., Pollack, J. B., and Hansen, G. B. (1995). Low brightness temperatures of Martian polar caps : CO_2 clouds or low spectral emissivity? *J. Geophys. Res.*, 100:21,119–21,234.

[Haberle et al., 1993] Haberle, R. M., Pollack, J. B., Barnes, J. R., Zurek, R. W., Leovy, C. B., Murphy, J. R., Lee, H., and Schaeffer, J. (1993). Mars atmospheric dynamics as simulated by the NASA/Ames general circulation model I. the zonal-mean circulation. *J. Geophys. Res.*, 98(E2):3093–3124.

[Hourdin, 1992] Hourdin, F. (1992). A new representation of the CO_2 15μm band for a Martian general circulation model. *J. Geophys. Res.*, 97(E11):18,319–18,335.

[Hourdin et al., 1995] Hourdin, F., Forget, F., and Talagrand, O. (1995). The sensitivity of the Martian surface pressure to various parameters: Acomparison between numerical simulations and Viking observations. *J. Geophys. Res.*, 100:5501–5523.

[Hourdin et al., 1993] Hourdin, F., Le Van, P., Forget, F., and Talagrand, O. (1993). Meteorological variability and the annual surface pressure cycle on Mars. *J. Atmos. Sci.*, 50:3625–3640.

[Jaquin et al., 1986] Jaquin, F., Gierasch, P., and Kahn, R. (1986). The vertical structure of limb hazes in the Martian atmosphere. *Icarus*, 68:442–461.

[Joshi et al., 1994] Joshi, M. M., Lewis, S. R., Read, P. L., and Catling, D. C. (1994). Western boundary currents in the atmosphere of Mars. *Nature*, 367:548–551.

[Kieffer et al., 1977] Kieffer, H. H., Martin, T. Z., Peterfreund, R., Jakosky, B. M., Miner, E. D., and Palluconi, F. D. (1977). Thermal and albedo mapping during the Viking primary mission. *J. Geophys. Res.*, 82:4249–4291.

[Leovy and Mintz, 1969] Leovy, C. and Mintz, Y. (1969). Numerical simulation of the atmospheric circulation and climate of Mars. *J. Atmos. Sci.*, 26:1167–1190.

[Lott and Miller, 1996] Lott, F. and Miller, M. (1996). A new sub-gris scale orographic drag parametrization: its formulation and testing. *Q. J. R. Meteorol. Soc.*, In Press.

[Magalhaes, 1987] Magalhaes, J. A. (1987). The Martian Hadley circulation: Comparison of "viscous" predictions to observations. *Icarus*, 70:442–468.

[Martin, 1986] Martin, T. Z. (1986). Thermal infrared opacity of the Mars atmosphere. *Icarus*, 66:2–21.

[Mellor and Yamada, 1974] Mellor, G. L. and Yamada, T. (1974). A hierarchy of turbulence closure models for planetary boundary layers. *J. Atmos. Sci.*, 31:1791–1806.

[Miller et al., 1989] Miller, M. J., Palmer, P. M., and Swinbank, R. (1989). Parametrisation and influence of sub-grid scale orography in general circulation and numerical weather prediction models. *Meteor. & Atmos. Phys.*, 40:84–109.

[Ockert-Bell et al., 1997] Ockert-Bell, M. E., Bell III, J. F., McKay, C., Pollack, J., and Forget, F. (1997). Absorption and scattering properties of the martian dust in the solar wavelengths. In press, *J. of Geophysical Research.*

[Paige et al., 1994] Paige, D. A., Bachman, J. E., and Keegan, K. D. (1994). Thermal and albedo mapping of the polar regions of Mars using viking thermal mapper observations 1. North polar region. *J. Geophys. Res.*, 99:25959–25991.

[Paige and Keegan, 1994] Paige, D. A. and Keegan, K. D. (1994). Thermal and albedo mapping of the polar regions of mars : 2. south polar region. *J. Geophys. Res.*, 99:25993–26013.

[Palluconi and Kieffer, 1981] Palluconi, F. D. and Kieffer, H. H. (1981). Thermal inertia mapping of Mars from 60^oS to 60^oN volume = 45, year = 1981. *Icarus*, 45:415–426.

[Pleskot and Miner, 1982] Pleskot, L. K. and Miner, E. D. (1982). Time variability of Martian bolometric albedo. *Icarus*, 50:259–287.

[Pollack et al., 1981] Pollack, J. B., Leovy, C. B., Greiman, P. W., and Mintz, Y. (1981). A Martian General Circulation Model experiment with large topography. *J. Atmos. Sci.*, 38:3–29.

[Toon et al., 1989] Toon, O. B., McKay, C. P., Ackerman, T. P., and Santhanam, K. (1989). Rapid calculation of radiative heating rates and photodissociation rates in inhomogeneous multiple scattering atmospheres. *J. Geophys. Res.*, 94:16,287–16,301.

[Toon et al., 1977] Toon, O. B., Pollack, J. B., and Sagan, C. (1977). Physical properties of the particles composing the Martian dust storm of 1971-1972. *Icarus*, 30:663–696.

[Wilson and Hamilton, 1996] Wilson, R. W. and Hamilton, K. (1996). Comprehensive model simulation of thermal tides in the Martian atmosphere. *J. Atmos. Sci.*, 53:1290–1326.

[Zurek et al., 1992] Zurek, R. W., Barnes, J. R., Haberle, R. M., Pollack, J. B., Tillman, J. E., and Leovy, C. B. (1992). Dynamics of the atmosphere of Mars. In *Mars*, pages 835–933, Tucson, AR. University of Arizona Press, Tucson.